Regenerative Therapy 19 (2022) 35–46

Contents lists available at ScienceDirect

Regenerative Therapy

journal homepage: http://www.elsevier.com/locate/reth

Original Article

Phenotypic and functional properties of dedifferentiated fat cells derived from infrapatellar fat pad

Koji Tanimoto [a], Taro Matsumoto [b, *], Yuki Nagaoka [b], Tomohiko Kazama [b], Chii Yamamoto [b], Koichiro Kano [c], Masahiro Nagaoka [a], Shu Saito [a], Yasuaki Tokuhashi [a], Kazuyoshi Nakanishi [a]

[a] Department of Orthopaedic Surgery, Nihon University School of Medicine, Tokyo, Japan
[b] Department of Functional Morphology, Division of Cell Regeneration and Transplantation, Nihon University School of Medicine, Tokyo, Japan
[c] Laboratory of Cell and Tissue Biology, Collage of Bioresource Science, Nihon University, Fujisawa, Japan

ARTICLE INFO

Article history:
Received 21 October 2021
Received in revised form
12 December 2021
Accepted 20 December 2021

Keywords:
Dedifferentiated fat cells
Adipose-derived stem cells
Infrapatellar fat pad
Adipocytes

ABSTRACT

Introduction: Mature adipocyte-derived dedifferentiated fat cells (DFATs) are mesenchymal stem cell (MSC)-like cells with high proliferative ability and multilineage differentiation potential. In this study, we first examined whether DFATs can be prepared from infrapatellar fat pad (IFP) and then compared phenotypic and functional properties of IFP-derived DFATs (IFP-DFATs) with those of subcutaneous adipose tissue (SC)-derived DFATs (SC-DFATs).

Methods: Mature adipocytes isolated from IFP and SC in osteoarthritis patients ($n = 7$) were cultured by ceiling culture method to generate DFATs. Obtained IFP-DFATs and SC-DFATs were subjected to flow cytometric and microarray analysis to compare their immunophenotypes and gene expression profiles. Cell proliferation assay and adipogenic, osteogenic, and chondrogenic differentiation assays were performed to evaluate their functional properties.

Results: DFATs could be prepared from IFP and SC with similar efficiency. IFP-DFATs and SC-DFATs exhibited similar immunophenotypes ($CD73^+$, $CD90^+$, $CD105^+$, $CD31^-$, $CD45^-$, $HLA\text{-}DR^-$) and tri-lineage (adipogenic, osteogenic, and chondrogenic) differentiation potential, consistent with the minimal criteria for defining MSCs. Microarray analysis revealed that the gene expression profiles in IFP-DFATs were very similar to those in SC-DFATs, although there were certain number of genes that showed different levels of expression. The proliferative activity in IFP-DFATs was significantly ($p < 0.05$) higher than that in the SC-DFATs. IFP-DFATs showed higher chondrogenic differentiation potential than SC-DFATs in regard to production of soluble galactosaminogalactan and gene expression of type II collagen.

Conclusions: IFP-DFATs showed higher cellular proliferative potential and higher chondrogenic differentiation capacity than SC-DFATs. IFP-DFAT cells may be an attractive cell source for chondrogenic regeneration.

Abbreviations: ASCs, adipose tissue-derived stem cells; BSA, bovine serum albumin; DEGs, differentially expressed genes; DFATs, dedifferentiated fat cells; DFs, dermal fibroblasts; FACS, fluorescence-activated cell sorting; FBS, fetal bovine serum; HLA, human leukocyte antigen; IFP, infrapatellar fat pad; MSCs, mesenchymal stem cells; OA, osteoarthritis; PBS, phosphate-buffered saline; PCA, principal component analysis; RT-PCR, reverse transcription-polymerase chain reaction; SC, subcutaneous adipose tissue; TBS, Tris-buffered saline; WST-1, water soluble tetrazolium-1.

* Corresponding author. Department of Functional Morphology, Division of Cell Regeneration and Transplantation, Nihon University School of Medicine, 30-1 Oyaguchi-Kamicho, Itabashi-ku, Tokyo 173-8610, Japan. Fax: +81-33972-8666.
E-mail address: matsumoto.taro@nihon-u.ac.jp (T. Matsumoto).

Peer review under responsibility of the Japanese Society for Regenerative Medicine.

https://doi.org/10.1016/j.reth.2021.12.006

1. Introduction

Articular cartilage defects have been considered difficult to repair because articular cartilage is an avascular tissue with a few cell components and has poor self-repair ability. When cartilage damage is left untreated, it frequently leads to osteoarthritis (OA) [1]. Autologous chondrocyte implantation has been widely used since the 1990s for the repair of articular cartilage defects, and it appears to be clinically useful [2,3]. However, autologous chondrocyte implantation is thought to be highly invasive because it requires two independent surgical procedures: cartilage collection from a healthy site and cell transplantation. In addition, it may be difficult to prepare a sufficient number of cells for transplantation in elderly patients. Furthermore, there is a risk of dedifferentiation of chondrocytes into fibroblast-like cells during long-term culture [4].

To overcome this problem, mesenchymal stem cells (MSCs) have attracted much attention as an alternative cell source to treat cartilage defects. MSCs can be isolated and expanded from a small amount of bone marrow or adipose tissue aspirates. As advantages of MSCs, tissue collection is less invasive compared to that for chondrocytes, and they can be transplanted safety in an undifferentiated state because they have no tumorigenic potential [5,6]. Many preclinical and clinical studies of MSC transplantation have been conducted for cartilage defects, and they have shown the efficacy and safety of cell transplantation [7,8]. Moreover, it has been reported that intra-articular injection of MSCs for knee OA resulted in better clinical outcomes compared to that of hyaluronic acid [9–12]. However, as a cell source for autologous cell therapy, MSCs are problematic in that their proliferative ability and therapeutic activity may change depending on donor age and underlying diseases [13,14]. Therefore, an optimal therapeutic cell source that shows stable performance without being affected by patient age and underlying diseases is still desired.

A previous work by Matsumoto et al. [15] reported that mature adipocyte-derived dedifferentiated fat cells (DFATs) exhibit high proliferative ability and multilineage differentiation potential, which are similar to those of MSCs. DFATs are a more homogeneous cell population than adipose tissue-derived stem cells (ASCs) and exhibit stable multilineage differentiation potential regardless of donor age and underlying diseases. DFAT transplantation has been shown to have therapeutic effects on animal models of various osteochondral diseases such as bone defects [16], cartilage defects [17], and intervertebral disc degeneration [18]. Thus, DFATs can be expected as an attractive cell source to treat knee OA, which is common in the elderly.

The infrapatellar fat pad (IFP) is located in the knee joint and is frequently excised and disposed of as medical waste during arthroscopy or open surgery on the knee. Recent studies showed that ASCs could be prepared from IFP [19]. Interestingly, IFP-derived ASCs exhibited greater cartilage differentiation ability compared to subcutaneous adipose tissue (SC)-derived ASCs [20–22].

Although DFATs may be prepared from IFP, there are, to our knowledge, no reports of it. In addition, the phenotypic properties and differentiation potential of IFP-derived DFATs are still unknown. In this study, we first examined whether DFATs can be prepared from IFP collected from OA patients, and then we compared phenotypic and functional properties of IFP-derived DFATs (IFP-DFATs) with those of SC-derived DFATs (SC-DFATs) using donor-matched tissue samples.

2. Materials and methods

2.1. Human tissue samples

IFP and SC were obtained from seven female patients (average age 70.6 ± 8.1 years, average body mass index 24.4 ± 3.7 kg/m^2) with knee OA (Kellgren-Lawrence grade III or IV) during total knee arthroplasty in the Department of Orthopedic surgery of Nihon University Itabashi Hospital (Tokyo, Japan). The SC was harvested from the medial side near the vastus medialis muscle. Patients with aggressive synovitis were excluded. Donors provided informed written consent for this study, which was approved by the Clinical Research Judging Committee of Nihon University Itabashi Hospital (Approval number RK-121012-3).

2.2. DFAT preparation

Preparation of IFP- and SC-DFATs using the ceiling culture method was described previously [23]. Briefly, approximately 1–2 g of SC and IFP fat tissue was minced and digested with 0.1% (W/V) type II collagenase solution (Sigma-Aldrich, St. Louis, MO) at 37 °C for 30 min. After filtration and centrifugation at 135×g for 1 min, the floating top layer containing unilocular adipocytes was collected. The cells were washed with phosphate-buffered saline (PBS), placed in a T-12.5 cell culture flask (NUNC, Roskilde, Denmark) filled with Dulbecco's Modified Eagle's Medium (DMEM, Invitrogen, Carlsbad, CA) containing 20% fetal bovine serum (FBS, Lot 6G2146; JRH Biosciences Inc., Lenexa, KS), and incubated at 37 °C under 5% CO_2. The cells floated up and adhered to the top inner ceiling surface of the flask. At 7 days after culturing, the medium was removed and the flasks were turned upside-down so that the cells were oriented on the bottom. The medium was exchanged every 3 or 4 days until the cells reached confluency. For passage, the cells were harvested by treating the cells with a trypsin-ethylenediaminetetraacetic acid solution (Invitrogen), following which the cells were seeded in 100-mm dishes at a density of 1×10^6 cells per dish and cultured. Cells at the second passage (P2) were used in the experiments.

2.3. Flow cytometry

DFATs suspended in autoMACS Running Buffer (Miltenyi Biotec, Bergish Gladbach, Germany) containing 0.2% bovine serum albumin (BSA) were adjusted to 1×10^6 cells per 100 μl. To inhibit non-specific binding, the cells were added to 10 μl normal rabbit serum (Lot 100M8400; Sigma-Aldrich) and left to stand for 10 min. After washing with autoMACS Running Buffer, 10 μl of various anti-human monoclonal antibodies were added, and the mixture was left to stand in the dark at 4 °C for 30 min. The following antibodies were used: phycoerythrin (PE)-labeled anti-human CD73, PE-labeled anti-human CD31, PE-labeled anti-human human leukocyte antigen (HLA)-DR, allophycocyanin (APC)-labeled anti-human CD90, APC-labeled anti-human CD105, and APC-labeled anti-human CD45 (all from BD Biosciences, San Jose, CA). PE- or APC-labeled anti-mouse immunoglobulin G (IgG) antibody (BD Biosciences) was used as the isotype control. After the antibody reaction, 500 μl of autoMACS Running Buffer was added to the sample, which was then transferred to a 5-ml fluorescence-activated cell sorting (FACS) round tube (BD Falcon, Franklin Lakes, NJ) through a mesh filter. To detect dead cells, 5 μl of 7-aminoactinomycin D (BD Biosciences) was added to each tube. For the measurement of cell surface antigens, a FACSAria flow cytometer (Becton Dickinson, Bedford, MA) was used. The 7-aminoactinomycin D-negative fraction was gated for forward scatter and side scatter, and only living cells were analyzed. Flow cytometry data was analyzed with FlowJo Version 9 software (FlowJo LLC, Ashland, OR).

2.4. Microarray analysis

Normal human dermal fibroblasts (DFs, n = 5) were purchased from Lonza (Walkersville, MD) and cultured according to the

manufacturer's protocol. Total ribonucleic acid (RNA) was extracted from SC-DFATs, IFP-DFATs, and DFs using an RNeasy Mini Kit (Qiagen, Hilden, Germany) according to the manufacturer's instructions. The quality of the extracted RNA was assessed using an Agilent 2100 Bioanalyzer (Agilent Technologies, Santa Clara, CA). The GeneChip™ 3′IVT PLUS Reagent Kit (Affymetrix Inc., Santa Clara, CA) was used for synthesis and purification of cDNA, in vitro transcription, and T7RNA amplification and labeling. Fragmentation of RNA was performed with the GeneChip™ Hybridization, Wash, and Stain Kit (Thermo Fisher Scientific, Waltham, MA). The RNA samples were hybridized to probes using GeneChip™ Human Genome U133 Plus 2.0 Array (Affymetrix) according to the manufacturer's instructions. Fluorescent images were visualized using a GeneChip™ Scanner 3000 (Affymetrix). Gene expression data were analyzed using Transcriptome Analysis Console software (Affymetrix) according to the software's guidelines. An adjusted p-value < 0.05 and log-FC $\geq \pm 2.0$ were set as the cut-off criteria to screen differentially expressed genes (DEGs). Gene Ontology enrichment analysis was performed on up-regulated or down-regulated DEGs using Metascope [24].

2.5. Cell proliferation assay

To evaluate the cellular proliferative potential of IFP-DFATs, a water soluble tetrazolium-1 (WST-1) assay was performed with Cell Proliferation Reagent WST-1 (Sigma-Aldrich) according to the attached protocol. Briefly, DFATs at P2 were seeded onto 24-well plates (BD Falcon) at a density of 2500 cells per well and cultured in DMEM containing 20% FBS. On days 2, 4, and 7 after culturing, the medium of each well was removed, and 110 μl of Cell Proliferation Reagent WST-1 was added. Similarly, empty wells were used as blanks. Then, the plates were left to stand for 30 min at 37 °C under 5% CO_2, and 100 μl of each cell solution was transferred to 96-well plates. Then, absorbance at 450 nm was measured with a microplate reader (iMark, Bio-Rad Laboratories, Hercules, CA). All samples were measured in triplicate. Population doubling time of the cultured cells was determined as described previously [25].

2.6. Adipogenic differentiation assay

DFATs at P2 were seeded on 24-well plates at a density of 6×10^4 cells per well and cultured in adipogenic differentiation medium (Mesenchymal Stem Cell Adipogenic Differentiation Medium 2: C-28016; PromoCell, Heidelberg, Germany). At 14 days of culture, samples were washed twice with PBS and fixed with 4% paraformaldehyde (PFA) for 60 min. After fixation, samples were washed twice with PBS and stained with Oil red O staining solution (Sigma Aldrich) for 20 min. After being washed three times with distilled water, samples were photographed with a VB-7000 stereoscopic microscope (Keyence, Osaka, Japan). After the staining, samples were dried and incubated with 100 μl of isopropyl alcohol for 10 min. Then, the solution was collected and absorbance at 490 nm was measured with the microplate reader (iMark). Each quantitative value was evaluated from the average value of the absorbance at two wells to subtract the value of the blank containing only isopropyl alcohol. In another experiment, DFAT samples at 14 days of culture were used for real-time reverse transcription-polymerase chain reaction (RT-PCR) analysis.

2.7. Osteogenic differentiation assay

DFATs at P2 were seeded on 24-well plates at a density of 6×10^4 cells per well and cultured in the osteogenic differentiation induction medium (Mesenchymal Stem Cell Osteogenic Differentiation Medium: C-28013; Promo Cell). At 14 days of culture, samples were washed twice with PBS and fixed with 4% PFA for 60 min. After fixation, samples were washed twice with PBS and stained with 1% Alizarin red S (Sigma Aldrich) for 3 min. After being washed three times with distilled water, samples were photographed with the VB-7000 stereoscopic microscope (Keyence). The intensity of Alizarin red S staining was quantified by modifying the method of Gregory et al. [26]. Briefly, 10% acetic acid was added to each well and incubated at room temperature for 30 min with shaking. Loosely attached cells were collected with a cell scraper and transferred to a 1.5-mL tube. After heating at 85 °C for 10 min, samples were centrifuged at 20,000×*g* for 15 min and the supernatant was collected. Then, 50 μl of 5% ammonia water (pH 4.1–4.5) was added, and the absorbance at 405 nm was measured with the microplate reader (iMark).

2.8. Chondrogenic differentiation assay

Induction of chondrogenic differentiation by the pellet culture method was used according to a previous report [17] with slight modification. Briefly, DFATs at P2 were seeded in a 15-ml polypropylene tube (BD Falcon) at density of 5×10^5 cells with 2 ml of chondrogenic differentiation induction medium (NH Chondrodiff Medium, Miltenyi Biotec). Cells were centrifuged at 500×*g* for 10 min to precipitate them and cultured at 37 °C under 5% CO_2. The medium was exchanged every 3 days. At 21 days of culture, the medium was removed, and the generated micromass pellets were fixed with 4% PFA for 60 min. After being washed with distilled water, the micromass pellets were photographed using the VB-7000 stereomicroscope (Keyence), and the weight of each micromass pellet was measured using an electronic analytical balance (AEG-45SM, Shimazu, Kyoto, Japan). The samples were then subjected to histological analysis and quantification analysis for glycosaminoglycans. In another experiment, DFAT samples at 0, 7, and 14 days of culture were used for RT-PCR analysis.

2.9. Histological evaluation

The cartilage-like micromass pellets were fixed with 4% PFA, dehydrated, and embedded in paraffin. Samples were sliced into 4-μm sections and stained with Toluidine Blue, Alcian Blue, and Safranin O. For aggrecan immunostaining, the sections were deparaffinized and incubated with 25 μg/ml hyaluronidase at 37 °C for 30 min and blocked with 10% goat serum and 1% BSA in Tris buffered saline (TBS) at room temperature for 1 h. The sections were incubated with rabbit anti-human aggrecan antibody (1:100 dilution, clone 13880-1-AP; Proteintech, Rocky Hill, NJ) at 4 °C overnight. After washing with TBS, the sections were incubated with peroxidase-conjugated anti-rabbit IgG antibody (1:200 dilution, DakoCytomation, Glostrup, Denmark) at room temperature for 30 min. For the peroxidase reaction, 0.3% 3,3′-diaminobenzidine tetrahydrochloride was used as the chromogenic substrate. The sample was observed with an upright microscope (BX51, Olympus, Tokyo, Japan) and photographed with a microscope digital camera (DP20-5, Olympus).

2.10. Real-time RT-PCR

The changes in the expression of mRNA in the adipogenic and chondrogenic differentiation of DFATs were evaluated by a real-time RT-PCR method with TaqMan probe. Total RNA was extracted from cells with an Isogen RNA Extraction kit (Nippon Gene Co., Tokyo, Japan). Then, total RNA was reverse transcribed into cDNA with a TaKaRa RNA PCR Kit (AMV) Ver. 3.0 (Takara Bio, Ohtsu, Japan). The

primers and the probes for *SOX9* (sry-box transcription factors 9) (Hs00165814_ml), *COL2A1* (type II collagen, Hs00194197_ml), *PPARG* (peroxisome proliferator activated receptor γ) (Hs00234592_ml), *ADIPOQ* (adiponectin, C1Q and collagen domain containing) (Hs00605917_ml), *LEP* (leptin, Hs00174877_ml), and *GLUT4* (glucose transporter 4) (Hs00168966_ml) were TaqMan Pre-Developed Assay Reagents (Applied Biosystems, Foster City, CA). mRNA was quantified with an ABI Prism 7300 (Applied Biosystems). Cycling parameters were 95 °C for 10 min followed by 40 cycles of 95 °C for 15 s and 60 °C for 1 min. Each sample was run in triplicate. Relative gene expression was analyzed by the comparative cycle threshold method with 18S ribosomal RNA (Hs99999901_s1, Applied Biosystems) as the endogenous control.

2.11. Quantification of glycosaminoglycans

The amounts of glycosaminoglycans in the cartilage-like micromass pellets were quantified as described previously [27]. Briefly, samples were digested with protease K at 56 °C for 15 h. The quantity of glycosaminoglycans was then measured spectrophotometrically using dimethylmethylene blue, with chondroitin sulfate as a standard.

2.12. Statistical analysis

The values shown in the graphs are expressed as mean ± standard error. Statistical analysis for comparison between groups was performed using the Mann-Whitney U test. A p value < 0.05 was considered to indicate statistical significance. GraphPad Prism Version 5 (GraphPad Software, La Jolla, CA) was used for statistical analysis.

3. Results

3.1. Preparation of DFATs from IFP

We first tried to prepare DFATs from mature adipocytes isolated from IFP by using ceiling culture. Histologically, adipose tissue in IFP consisted of various lobules defined by connective septa containing blood vessels and elastic fibers (Suppl. Fig. 1). The ceiling culture method is illustrated in Fig. 1a. When the isolated adipocytes were incubated in the ceiling culture, the cells attached to the upper surface of the flasks by day 2 of culture (Fig. 1b), subsequently colonies of spindle-shaped DFATs were observed by day 7 (Fig. 1b, arrows). After that, DFATs continued to grow and

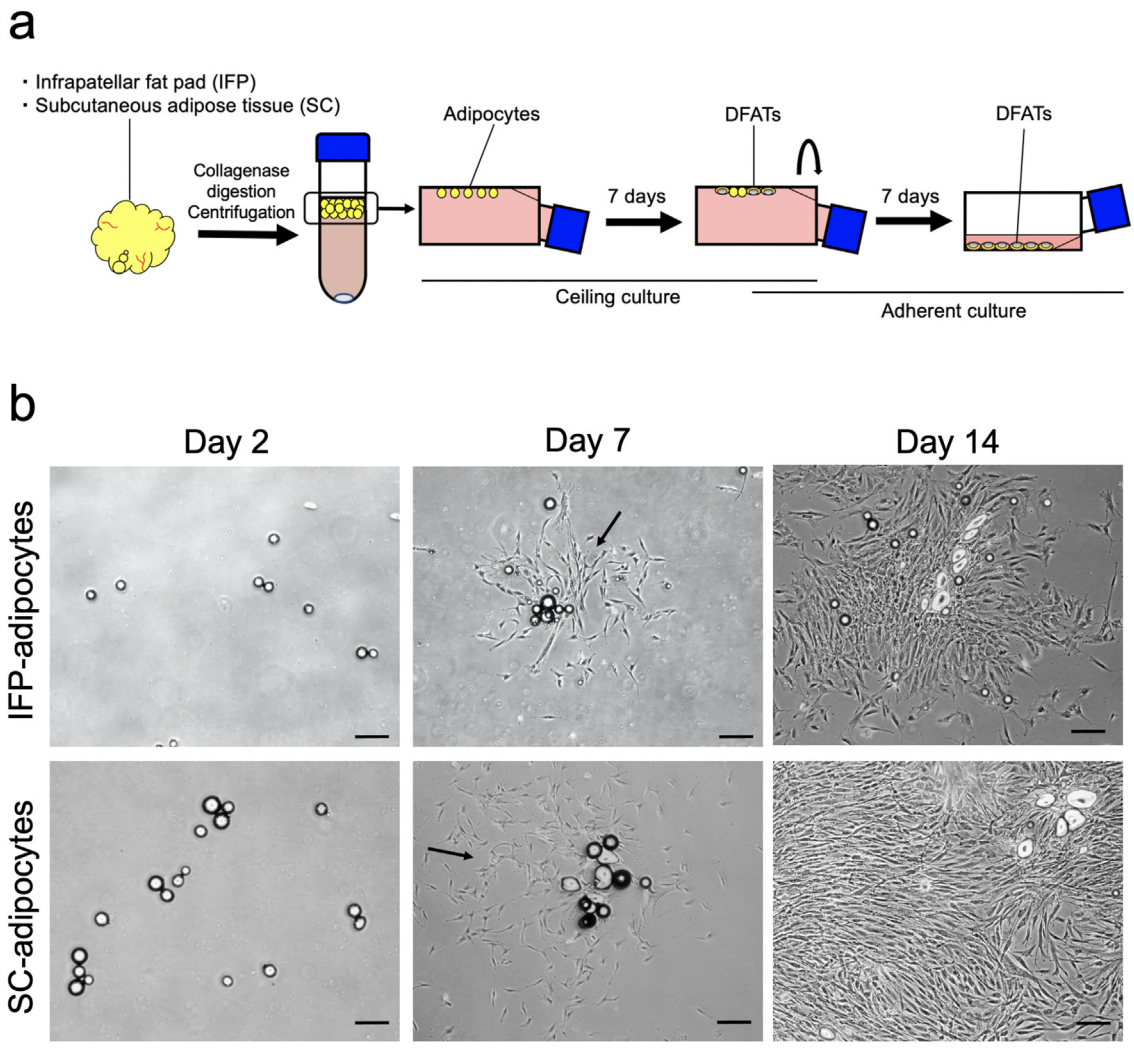

Fig. 1. Morphological changes of mature adipocytes during ceiling culture. Mature adipocytes isolated from infrapatellar fat pad (IFP) and subcutaneous adipose tissue (SC) were incubated in the ceiling culture. (a) Schematic illustration of the culture method used to prepare dedifferentiated fat cells (DFATs). (b) Morphological changes of IFP-adipocytes and SC-adipocytes during the ceiling culture are shown. Arrows indicate a colony of DFATs. Scale bars represent 100 μm.

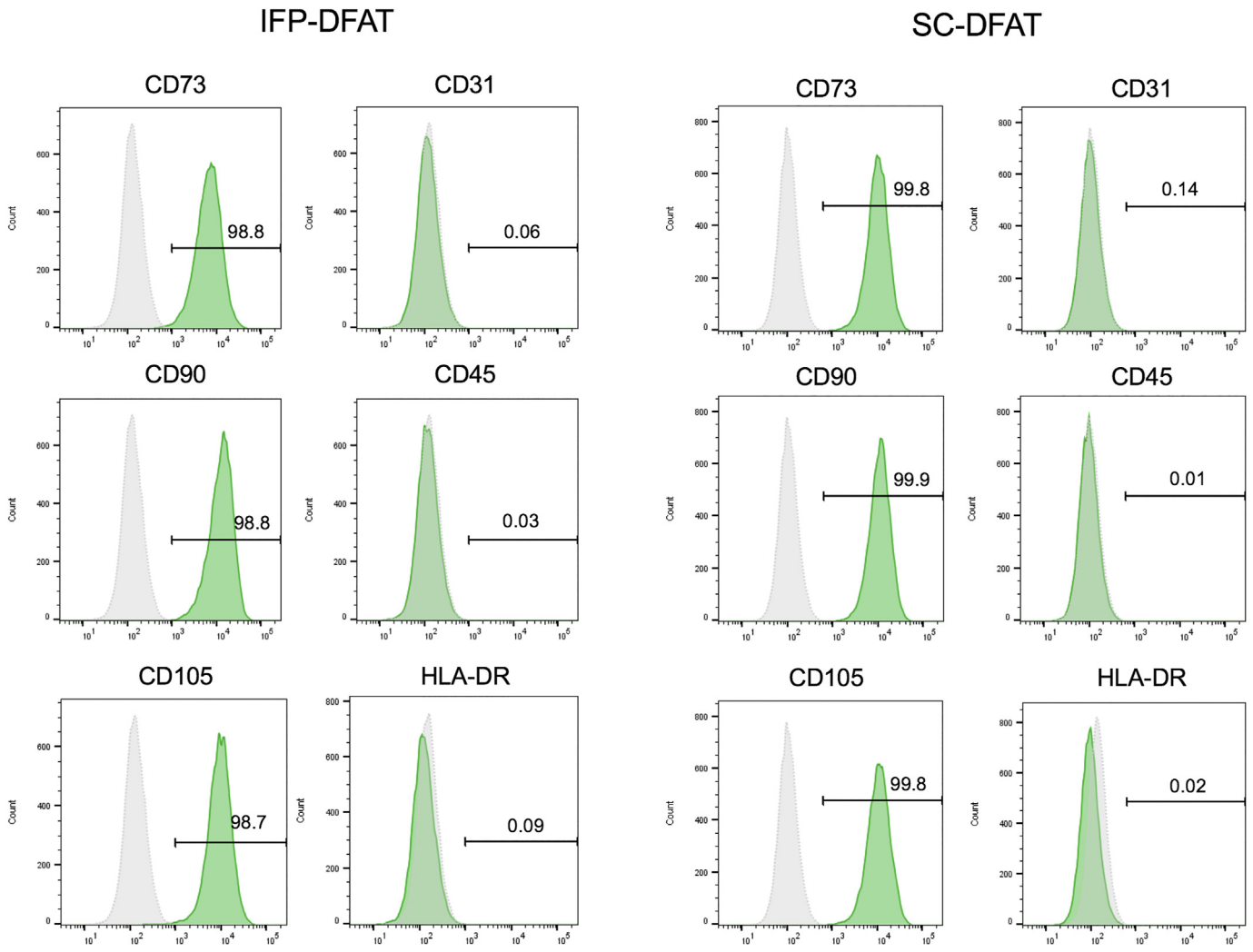

Fig. 2. Immunophenotypic analysis of IFP-DFATs and SC-DFATs. IFP-DFATs and SC-DFATs at passage 2 were subjected to flow cytometric analysis to determine their immunophenotypes. Green histograms represent target immunofluorescence, and grey histograms represent isotype control.

reached subconfluence at 14 days of culture. The morphological changes in the IFP-derived adipocytes during the ceiling culture were very similar to those in the SC-derived adipocytes. Similar results were repeatedly observed from all tissue samples examined (n = 7). These findings indicated that DFATs can be prepared from IFP-derived adipocytes in a similar way as SC-derived adipocytes.

3.2. Immunophenotype of IFP-DFATs

We next compared the cell-surface antigen profiles of IFP-DFATs with SC-DFATs at P2. Flow cytometric analysis showed that IFP-DFATs and SC-DFATs were more than 98% positive for MSC markers CD73, CD90, and CD105 (Fig. 2). Neither type of DFATs expressed MSC negative markers CD31, CD45, and HLA-DR at less than 0.15%. These results suggested that IFP-DFATs exhibited a similar immunophenotype as that of SC-DFATs, which is consistent with the immunophenotype of MSCs.

3.3. Gene expression profile of IFP-DFATs

We next examined the microarray analysis to clarify the differences in gene expression profiles between IFP-DFATs and SC-DFATs. Principal component analysis revealed that IFP-DFATs were transcriptionally similar to SC-DFATs and that both types of DFATs were transcriptionally distinct compared to DFs (Fig. 3a). In total, 3317 (6.07%) and 4662 (8.54%) genes were found to be significantly ($p < 0.05$ and log-FC $\geq \pm 2.0$) differentially regulated in the DFs vs SC-DFATs and DFs vs IFP-DFATs comparisons, respectively (Fig. 3b). In contrast, a much smaller number of 539 genes (0.99%) were identified in the IFP-DFATs and SC-DFATs comparison, suggesting high similarity in gene expression profiles between IFP-DFATs and SC-DFATs. Heatmap analysis revealed that the gene expression profiles in IFP-DFATs from four different individuals were involved in a same cluster and separated from those in SC-DFATs (Fig. 3c). The significantly up-regulated and down-regulated DEGs in IFP-DFATs compared with SC-DFATs are listed in Supplementary Table 1, the fold change of which ranged from −5 to 5. Gene Ontology analysis revealed that significant gene ontology terms of up-regulated DEGs in IFP-DFATs included response to growth factor (GO-0070848), developmental growth (GO-0048589), and skeletal system development (GO-0001501), whereas those of down-regulated DEGs included integrin cell surface interactions (R-HAS-216083), response to wounding (GO-0009611), and positive regulation of extrinsic apoptotic signaling pathway via death domain receptors (GO-1902043) (Fig. 3d). These findings indicated that the

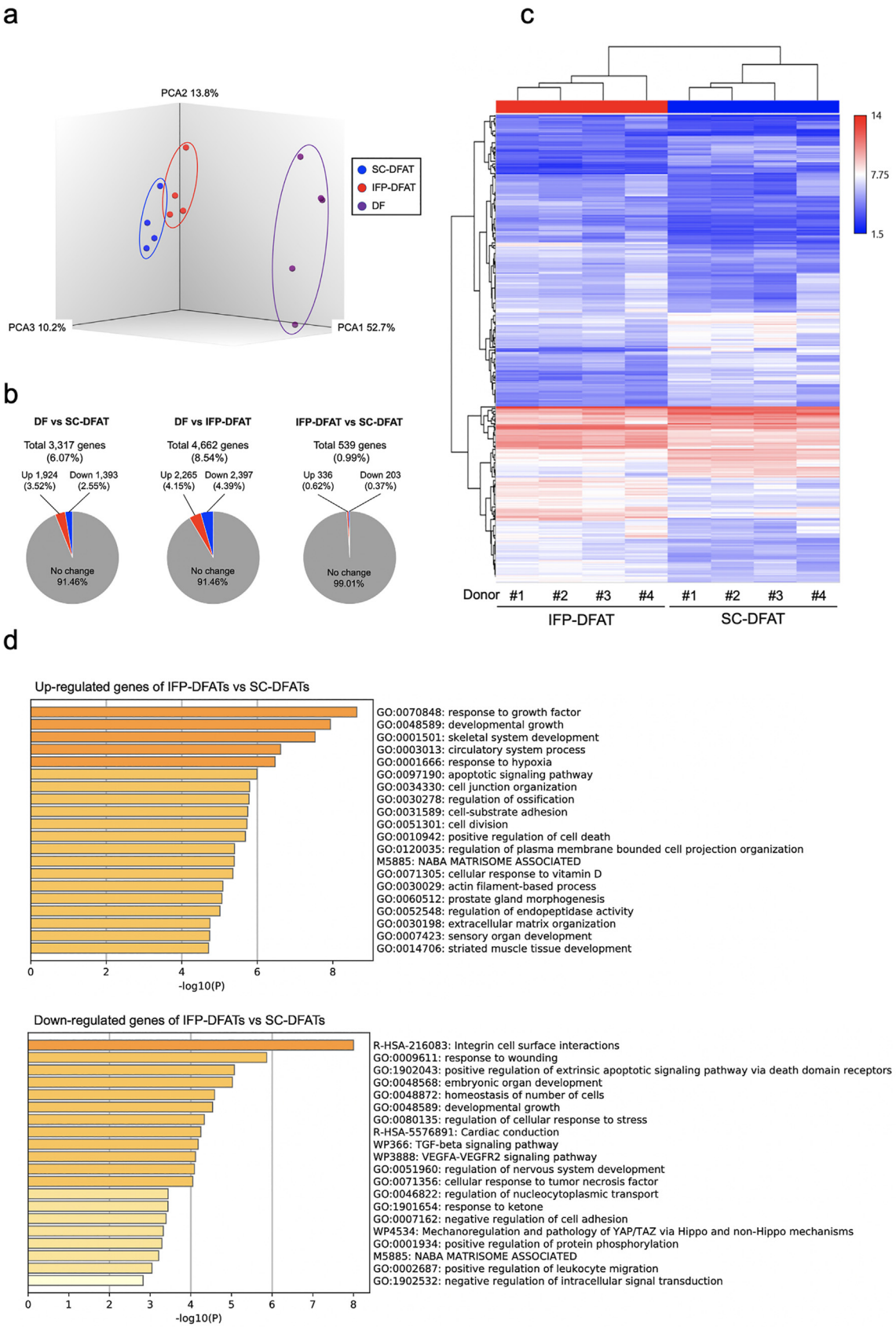

Fig. 3. Microarray analysis of IFP-DFATs and SC-DFATs. Total RNA was extracted from IFP-DFATs (n = 4), SC-DFATs (n = 4), and dermal fibroblasts (DFs, n = 5) and subjected to microarray analysis. (a) Principal component analysis (PCA) plot of IFP-DFAT, SC-DFAT, and DF samples. (b) Number and percentage of differentially expressed genes (DEGs) between each pairwise comparison for IFP-DFATs, SC-DFATs, and DFs. (c) Heat map of DEGs in IFP-DFATs and SC-DFATs. (d) Top significant enriched Gene Ontology terms of the up-regulated and down-regulated DEGs in IFP-DFATs compared to SC-DFATs.

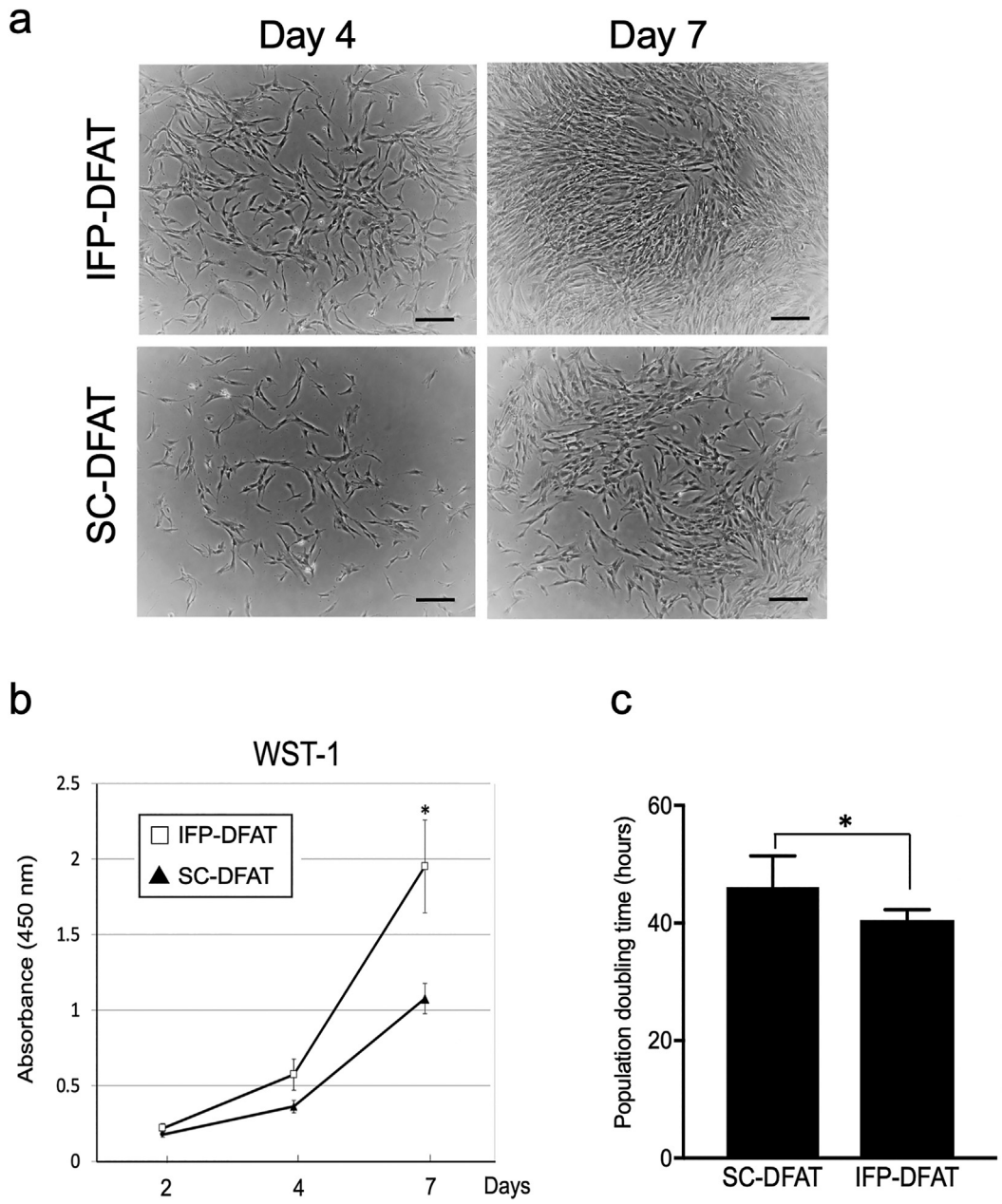

Fig. 4. Cell proliferation analysis of IFP-DFATs and SC-DFATs. IFP-DFATs and SC-DFATs (2500 cells/well, each n = 4) were cultured for 7 days and subjected to WST-1 assay to evaluate their cell proliferation ability. (a) Representative photomicrographs of the morphology of each type of cells. Scale bars represent 100 μm. (b) Evaluation of proliferative ability by WST-1 assay for each type of cells. Data are presented as mean ± SE. *p < 0.05 vs SC-DFAT. (c) Population doubling time of each type of cells. Data are presented as mean ± SD. *p < 0.05.

gene expression profiles in IFP-DFATs are very similar with those in SC-DFATs, although there are certain number of genes that showed different levels of expression.

3.4. Proliferative potential of IFP-DFATs

We next compared the proliferative potential of SC-DFATs with that of IFP-DFATs prepared from the donor-matched samples (n = 4). Microscopic analysis showed that the number of IFP-DFATs was greater than that of SC-DFATs at 4 days of culture, and the differences were prominent at 7 days (Fig. 4a). The WST-1 assay revealed that the proliferative activity in IFP-DFATs was significantly ($p < 0.05$) higher than that in the SC-DFATs at 7 days of culture (Fig. 4b). The population doubling time of IFP-DFATs (40.5 ± 1.8 h) was significantly ($p < 0.05$) shorter than that of SC-DFATs (46.1 ± 5.3 h) (Fig. 4c). The results indicated that the IFP-DFATs possess relatively higher proliferative potential compared to SC-DFATs.

3.5. Adipogenic differentiation potential of IFP-DFATs

We next examined the in vitro adipogenic differentiation potential of IFP-DFATs. After adipogenic induction, Oil red-O staining revealed that numerous lipid droplets were observed in both SC-DFATs and IFP-DFATs (Fig. 5a). Quantitative analysis showed there were similar intensity levels of Oil red O staining between IFP-

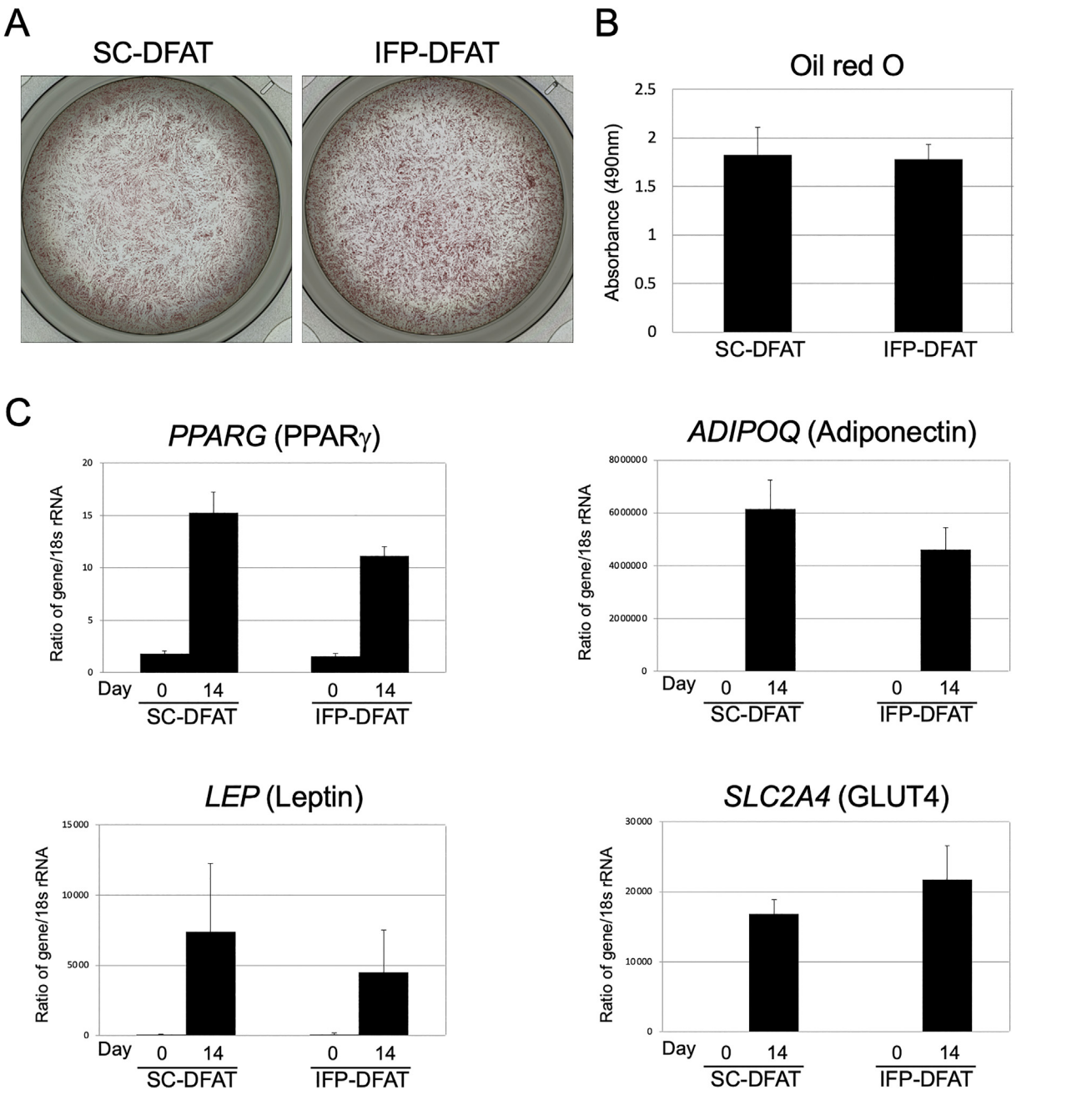

Fig. 5. Adipogenic differentiation potential of IFP-DFATs and SC-DFATs. SC-DFATs and IFP-DFATs (P2, each n = 6) were cultured for 14 days in adipogenic differentiation medium. Then, the cells were stained with Oil red O and were evaluated for adipogenic marker genes expression by RT-PCR. (a) Representative images of Oil red O staining in each type of cells. (b) Quantification of eluted neutral fat amounts in each type of cells. Data are represented as mean ± SE. (c) Expression of adipogenic marker genes before (Day 0) and after (Day 14) the induction in each type of cells. Data are presented as mean ± SE.

DFATs and SC-DFATs (Fig. 5b). Real-time RT-PCR analysis revealed that expression of *PPARG*, a commitment marker for adipocyte lineages, was observed in both types of DFATs before adipogenic induction (Day 0), and their expression was increased by more than 10-fold at 14 days after induction (Fig. 5c). The expression of mature adipocyte markers *ADIPOQ*, *LEP*, and *GLUT4* in both types of DFATs was also increased after induction. Statistical analysis revealed no significant difference in the expression levels of these markers between IFP-DFATs and SC-DFATs. These results indicated that IFP-DFATs possess adipogenic differentiation potential at a similar level to that of SC-DFAT cells.

3.6. Osteogenic differentiation potential of IFP-DFATs

We next compared the osteogenic differentiation potential of IFP-DFATs with that of SC-DFATs. Alizarin red S staining performed to visualize calcified deposits in cells revealed that both types of DFATs were mostly positive for Alizarin red S throughout the wells (Fig. 6a). The quantitative evaluation of Alizarin red S staining intensity showed no significant difference between them although the intensity of IFP-DFATs tended to be higher than that of SC-DFATs (Fig. 6b). The results confirmed that IFP-DFATs have osteogenic differentiation potential in vitro.

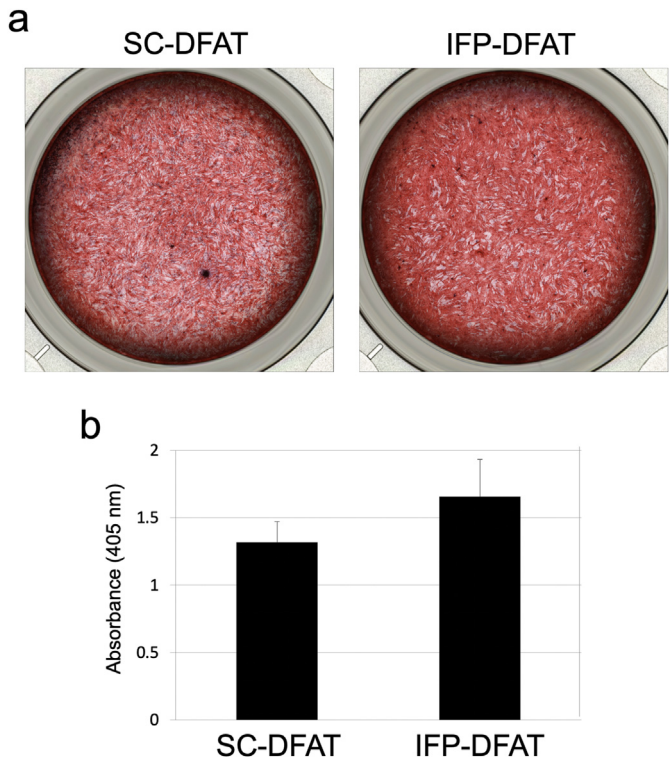

Fig. 6. Osteogenic differentiation potential of IFP-DFATs and SC-DFATs. SC-DFATs and IFP-DFATs (P2, each n = 4) were cultured for 14 days in osteogenic differentiation medium. Then, the cells were stained with Alizarin red S. (a) Representative images of Alizarin red S staining in each type of cells. (b) Quantification of the intensity of Alizarin red S in each type of cells. Data are presented as mean ± SE.

3.7. Chondrogenic differentiation potential of IFP-DFATs

We next compared the chondrogenic differentiation potential of IFP-DFATs with that of SC-DFATs. At 21 days after chondrogenic induction by pellet culture, the formation of cartilage-like micromass pellets of diameters of 1.5–2.0 mm was observed in both IFP-DFATs and SC-DFATs (Fig. 7a). The weights of the IFP-DFAT pellets tend to greater than those of the SC-DFAT pellets, although there was no significant difference between them due to large individual differences (Fig. 7b).

Histological analysis of the micromass pellets revealed that cartilage-specific extracellular matrix stained with Toluidine blue, Alcian blue, and Safranin O was observed in both the SC- and IFP-DFAT-derived micromass pellets (Fig. 7c). The positive area and intensity of these stainings in the IFP-DFAT-derived pellets tended to be stronger compared to those in the SC-DFAT-derived pellets. Immunostaining for aggrecan revealed that positive immunoreactivity was observed mainly on the surface of the cell masses in the IFP-DFAT-derived pellets, whereas relatively weaker immunoreactivity was detected in the SC-DFAT-derived pellets (Fig. 7c). Quantification analysis of glycosaminoglycans, a main component of the extracellular matrix of cartilage, revealed that the amounts of glycosaminoglycans in the IFP-DFAT-derived pellets were significantly ($p < 0.05$) greater than those in the SC-DFAT-derived pellets (Fig. 7d). Real-time RT-PCR analysis revealed that the expression of *SOX9*, a marker of the early stage of chondrogenesis, was increased at similar levels by 7 days after the chondrogenic differentiation culture in both IFP-DFATs and SC-DFATs (Fig. 7e). The expression of type II collagen (*COL2A1*), a marker of the terminal stage of chondrogenesis, was markedly increased at 14 days after the differentiation culture in IFP-DFATs, whereas the change in expression was less in SC-DFATs (Fig. 7f). Statistical analysis confirmed that the expression level of *COL2A1* in IFP-DFATs at 14 days was significantly ($p < 0.05$) greater than that in SC-DFATs. These results suggested that IFP-DFATs have higher chondrogenic differentiation potential than SC-DFATs.

4. Discussion

In the present study, we showed for the first time, to our knowledge, that DFATs can be generated from both IFP-derived adipocytes and SC-derived adipocytes. IFP-DFATs and SC-DFATs displayed similar immunophenotypes ($CD73^+$, $CD90^+$, $CD105^+$, $CD31^-$, $CD45^-$, $HLA\text{-}DR^-$) and tri-lineage (adipogenic, osteogenic, and chondrogenic) differentiation potential, consistent with the minimal criteria for defining MSCs [28]. Our previous studies showed that SC-DFATs have a higher homogeneous population with almost no MSC negative marker-expressing cells compared to ASCs [15,29]. The present study confirmed that IFP-DFATs were also highly homogeneous because of the very low frequency (<0.1%) of the MSC negative marker-expressing cells. Tangchitphisut et al. [30] reported that the percentage of negative marker-expressing cells in IFP-derived ASCs (IFP-ASCs) ranged from 0.17 to 1.24%, suggesting that they are a more heterogenous cell population than IFP-DFATs in the present study. Our microarray analysis showed that the gene expression profiles in IFP-DFATs are very similar to those in SC-DFATs (99.01% identical), suggesting high phenotypic similarity between them. Of note, our heatmap analysis revealed that gene expression profiles in IFP-DFATs from four different individuals were categorized in a cluster and distinguished from those in SC-DFATs, even though the two types of DFATs were from donor-matched adipocytes. These findings suggest that the gene expression profile of DFATs is defined in a site-dependent manner. To support this, a previous study showed that adipogenic progenitors in different depots of adipose tissue are intrinsically different and are programmed through epigenetic modulation early in their development [31].

Our results indicated that the IFP-DFATs possess relatively higher proliferative potential compared to SC-DFATs. Similarly, Garcia et al. [32] reported that the proliferation capacity of IFP-ASCs was greater than that of ASCs from donor-matched SC. IFP-ASCs from OA patients showed stable proliferative potential without signs of replicative senescence or transformation during long culture passages [33]. As the microenvironments of IFP from OA patients are different from those of SC in terms of a more inflammatory state of the IFP microenvironment, it is possible that IFP-derived adipocytes are transformed to mitotic phenotype in response to stimulation of surrounding immune cells. In support of this hypothesis, we found Gene Ontology terms associated with cell growth such as response to growth factor (GO-0070848), developmental growth (GO-0048589), and cell division (GO-0051301) as the top significantly enriched Gene Ontology terms of the up-regulated DEGs in IFP-DFATs (Fig. 3d).

Regarding the differentiation potential, IFP-DFATs showed tri-lineage differentiation potential similar to that of SC-DFATs. Interestingly, our results showed that IFP-DFATs have higher chondrogenic differentiation potential than SC-DFATs regarding the gene expression of type II collagen and the amounts of glycosaminoglycans after stimulation of chondrogenic differentiation. We found that the expression level of type II collagen in IFP-DFATs varied in each donor (Fig. 7f), and the level was not associate with pellet size and weight but correlate with the degree of cartilage-specific extracellular matrix accumulation in pellets. Similarly, previous reports showed that IFP-ASCs had higher chondrogenic differentiation potential compared to bone marrow MSCs and offer broad prospects in the treatment of osteoarthritis [34]. These findings

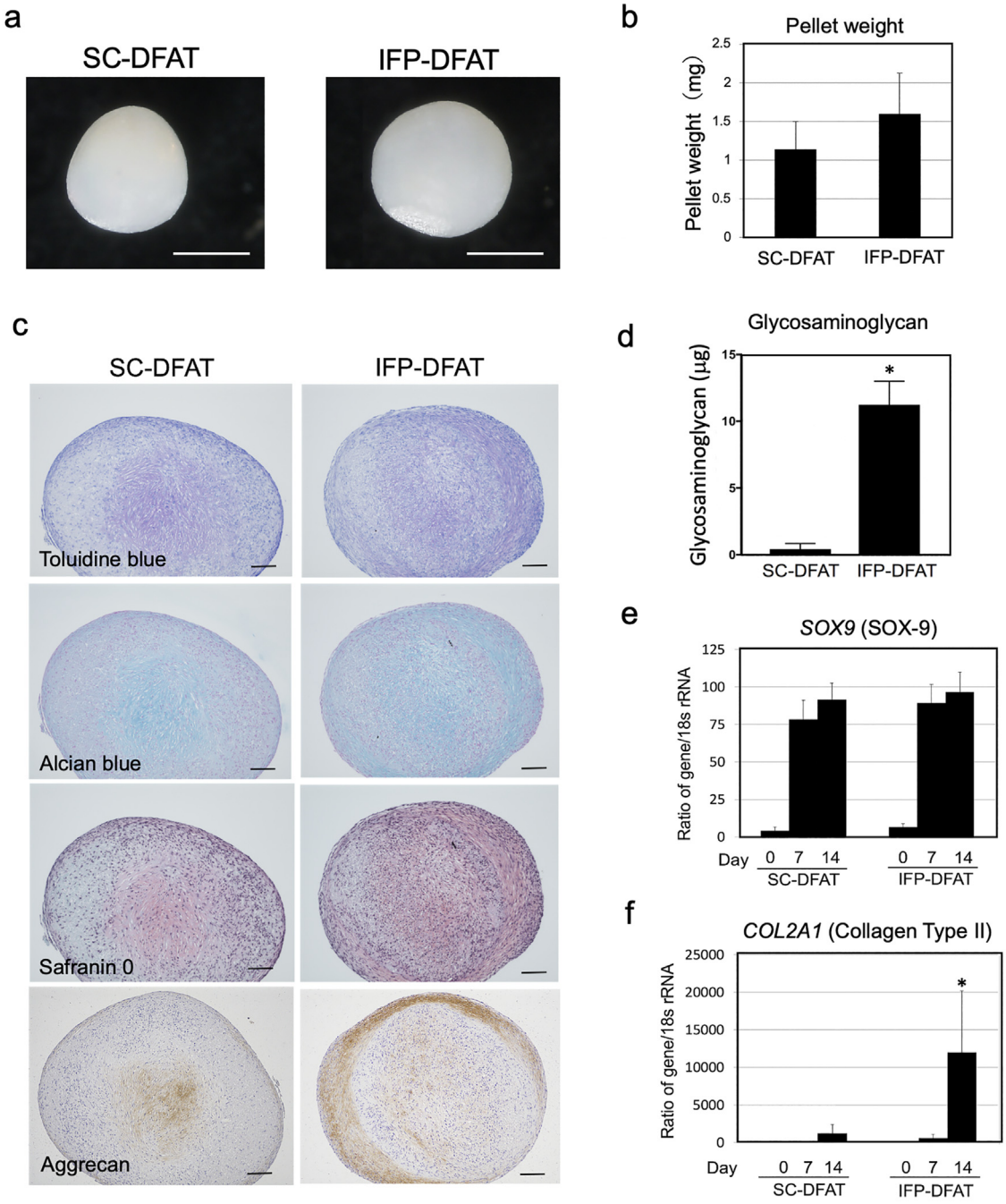

Fig. 7. Chondrogenic differentiation potential of IFP-DFATs and SC-DFATs. SC-DFATs and IFP-DFATs (P2, each n = 7) were seeded in 15-cm^3 conical tubes and cultured in chondrogenic medium for 21 days. Then, the formed cartilage-like micromass pellets were analyzed. (a) Representative morphology of the micromass pellets in each type of cells. Scale bars represent 1 mm. (b) Average weights of the micromass pellets in each type of cells. Data are presented as mean ± SE. (c) Representative photomicrographs of sectioned specimens of the micromass pellets stained with Toluidine blue, Alcian blue, Safranin O, and immunostained for aggrecan. Scale bars represent 200 μm. (d) Quantification of soluble glycosaminogalactan in each type of cells. *p < 0.05 vs SC-DFAT. (e, f) Expression of chondrogenic marker genes in each type of cells was measured by RT-PCR. The expressions of *SOX9* (e) and *COL2A1* (f) are shown. Data are presented as mean ± SE. *p < 0.05 vs SC-DFAT.

together with our results suggest that IFP-DFATs are also suitable for use in cartilage tissue engineering. The molecular mechanisms of the high differentiation property for chondrogenic lineage in IFP-DFATs are still unclear. We previously reported that DFATs prepared from buccal fat pad showed higher osteogenic differentiation potential compared to SC-DFATs [35]. It is possible that DFATs have originated tissue-dependent differences in their differentiation ability.

DFATs exhibit greater homogeneity than ASCs because DFATs are generated from mature adipocytes, which can be isolated from collagenase-digested adipose tissue with high purity by using their property of floating [15,29]. Although IFP contains a variety of blood cells and vascular cells, IFP-DFATs are expected to be a highly homogenous cell population and exhibit stable therapeutic potential. In addition, donor age and underlying disease do not appear to affect the proliferation and multilineage differentiation potential of

DFATs [15]. Indeed, the IFP-DFATs examined in this study were all from elderly individuals (average age 70.6 ± 8.1 years). Taken together, it is expected that autologous cell therapy using IFP-DFATs will show high effectiveness for elderly patients with knee OA. In the present study, one donor was significantly older (87 years) than the other donors (64–75 years). Interestingly, this donor-derived DFATs showed a slightly different gene expression profile in the microarray analysis (donor #4 in Fig. 3c) and relatively lower chondrogenic differentiation ability compared to the other donors-derived DFATs. In the case of very elderly patients, donor aging may influence phenotype and function of DFATs.

There are some limitations to the present study. First, all of the adipose tissue samples examined came from OA patients. Samples from healthy individuals should be tested to make a more precise comparison between the two types of DFATs. Second, differences of phenotypic and functional properties between IFP-DFATs and IFP-ASCs are still unclear since we did not analyze IFP-ASCs in the present study. Because we reported that SC-DFATs had several advantages in terms of their purity and functional properties compared to ASCs, further studies will be needed to clarify which type of cells is more suitable for cell-based therapies. Third, we did not examine any in vivo transplantation experiments using IFP-DFATs. To confirm the therapeutic potential of IFP-DFATs, in vivo transplantation studies will be needed using an appropriate animal disease model.

5. Conclusion

We showed that DFATs could be prepared from IFP in patients with OA. IFP-DFATs showed higher proliferative potential and higher chondrogenic differentiation capacity than did SC-DFATs. These results indicate that IFP-DFATs may be an attractive cell source for chondrogenic regeneration.

Declaration of competing interest

The authors declare that there is no conflict of interests in this article.

Acknowledgements

We thank Minako Kazama for assistance with flow cytometry. This research was supported by JSPS KAKENHI Grant Numbers 20H03581 and 17H04152, by AMED-supported Program for the Research Project for Practical Applications of Regenerative Medicine (21bk0104121h0001), by Nihon University President Grant Initiative (2018–2020), and by The Research Grant from the Chairperson and the President of Nihon University (2021–2022).

Appendix A. Supplementary data

Supplementary data to this article can be found online at https://doi.org/10.1016/j.reth.2021.12.006.

References

[1] Gelber AC, Hochberg MC, Mead LA, Wang NY, Wigley FM, Klag MJ. Joint injury in young adults and risk for subsequent knee and hip osteoarthritis. Ann Intern Med 2000;133(5):321–8.
[2] Brittberg M, Lindahl A, Nilsson A, Ohlsson C, Isaksson O, Peterson L. Treatment of deep cartilage defects in the knee with autologous chondrocyte transplantation. N Engl J Med 1994;331(14):889–95.
[3] Marcacci M, Kon E, Zaffagnini S, Filardo G, Delcogliano M, Neri MP, et al. Arthroscopic second generation autologous chondrocyte implantation. Knee Surg Sports Traumatol Arthrosc 2007;15(5):610–9.
[4] Yasui N, Osawa S, Ochi T, Nakashima H, Ono K. Primary culture of chondrocytes embedded in collagen gels. Exp Cell Biol 1982;50(2):92–100.
[5] Petersen BE, Bowen WC, Patrene KD, Mars WM, Sullivan AK, Murase N, et al. Bone marrow as a potential source of hepatic oval cells. Science 1999;284(5417):1168–70.
[6] Pittenger MF, Mackay AM, Beck SC, Jaiswal RK, Douglas R, Mosca JD, et al. Multilineage potential of adult human mesenchymal stem cells. Science 1999;284(5411):143–7.
[7] Kouroupis D, Kyrkou A, Triantafyllidi E, Katsimpoulas M, Chalepakis G, Goussia A, et al. Generation of stem cell-based bioartificial anterior cruciate ligament (ACL) grafts for effective ACL rupture repair. Stem Cell Res 2016;17(2):448–57.
[8] Park YB, Ha CW, Lee CH, Yoon YC, Park YG. Cartilage regeneration in osteoarthritic patients by a composite of allogeneic umbilical cord blood-derived mesenchymal stem cells and hyaluronate hydrogel: results from a clconcept with 7 years of extended follow-up. Stem Cells Transl Med 2017;6(2):613–21.
[9] Lamo-Espinosa JM, Mora G, Blanco JF, Granero-Moltó F, Nunez-Córdoba JM, Lopez-Elío S, et al. Intra-articular injection of two different doses of autologous bone marrow mesenchymal stem cells versus hyaluronic acid in the treatment of knee osteoarthritis: long-term follow up of a multicenter randomized controlled clinical trial (phase I/II). J Transl Med 2018;16(1):213.
[10] Jo CH, Lee YG, Shin WH, Kim H, Chai JW, Jeong EC, et al. Intra-articular injection of mesenchymal stem cells for the treatment of osteoarthritis of the knee: a proof-of-concept clinical trial. Stem Cells 2014;32(5):1254–66.
[11] Jayaram P, Ikpeama U, Rothenberg JB, Malanga GA. Bone marrow-derived and adipose-derived mesenchymal stem cell therapy in primary knee osteoarthritis: a narrative review. PM R 2019;11(2):177–91.
[12] Vega A, Martín-Ferrero MA, Del Canto F, Alberca M, García V, Munar A, et al. Treatment of knee osteoarthritis with allogeneic bone marrow mesenchymal stem cells: a randomized controlled trial. Transplantation 2015;99(8):1681–90.
[13] Gimble JM, Bunnell BA, Chiu ES, Guilak F. Concise review: adipose-derived stromal vascular fraction cells and stem cells: let's not get lost in translation. Stem Cells 2011;29(5):749–54.
[14] Zhang ZY, Teoh SH, Hui JH, Fisk NM, Choolani M, Chan JK. The potential of human fetal mesenchymal stem cells for off-the-shelf bone tissue engineering application. Biomaterials 2012;33(9):2656–72.
[15] Matsumoto T, Kano K, Kondo D, Fukuda N, Iribe Y, Tanaka N, et al. Mature adipocyte-derived dedifferentiated fat cells exhibit multilineage potential. J Cell Physiol 2008;215(1):210–22.
[16] Kikuta S, Tanaka N, Kazama T, Kazama M, Kano K, Ryu J, et al. Osteogenic effects of dedifferentiated fat cell transplantation in rabbit models of bone defect and ovariectomy-induced osteoporosis. Tissue Eng Part A 2013;19(15–16). 1792–802.
[17] Shimizu M, Matsumoto T, Kikuta S, Ohtaki M, Kano K, Taniguchi H, et al. Transplantation of dedifferentiated fat cell-derived micromass pellets contributed to cartilage repair in the rat osteochondral defect model. J Orthop Sci 2018;23(4):688–96.
[18] Nakayama E, Matsumoto T, Kazama T, Kano K, Tokuhashi Y. Transplantation of dedifferentiation fat cells promotes intervertebral disc regeneration in a rat intervertebral disc degeneration model. Biochem Biophys Res Commun 2017;493(2):1004–9.
[19] Liou JJ, Rothrauff BB, Alexander PG, Tuan RS. Effect of platelet-rich plasma on chondrogenic differentiation of adipose- and bone marrow-derived mesenchymal stem cells. Tissue Eng Part A 2018;24(19–20):1432–43.
[20] Dragoo JL, Samimi B, Zhu M, Hame SL, Thomas BJ, Lieberman JR, et al. Tissue-engineered cartilage and bone using stem cells from human infrapatellar fat pads. J Bone Joint Surg Br 2003;85(5):740–7.
[21] Lopez-Ruiz E, Perán M, Cobo-Molinos J, Jiménez G, Picón M, Bustamante M, et al. Chondrocytes extract from patients with osteoarthritis induces chondrogenesis in infrapatellar fat pad-derived stem cells. Osteoarthritis Cartilage 2013;21(1):246–58.
[22] Hindle P, Khan N, Biant L, Péault B. The infrapatellar fat pad as a source of perivascular stem cells with increased chondrogenic potential for regenerative medicine. Stem Cells Transl Med 2017;6(1):77–87.
[23] Sugihara H, Yonemitsu N, Miyabara S, Yun K. Primary cultures of unilocular fat cells: characteristics of growth in vitro and changes in differentiation properties. Differentiation 1986;31(1):42–9.
[24] Zhou Y, Zhou B, Pache L, Chang M, Khodabakhshi AH, Tanaseichuk O, et al. Metascape provides a biologist-oriented resource for the analysis of systems-level datasets. Nat Commun 2019;10(1):1523.
[25] Pokrywczynska M, Maj M, Kloskowski T, Buhl M, Balcerczyk D, Jundzill A, et al. Molecular aspects of adipose-derived stromal cell senescence in a long-term culture: a potential role of inflammatory pathways. Cell Transplant 2020;29.963689720917341.
[26] Gregory CA, Gunn WG, Peister A, Prockop DJ. An Alizarin red-based assay of mineralization by adherent cells in culture: comparison with cetylpyridinium chloride extraction. Anal Biochem 2004;329(1):77–84.
[27] Grogan SP, Barbero A, Winkelmann V, Rieser F, Fitzsimmons JS, O'Driscoll S, et al. Visual histological grading system for the evaluation of in vitro-generated neocartilage. Tissue Eng 2006;12(8):2141–9.
[28] Dominici M, Le Blanc K, Mueller I, Slaper-Cortenbach I, Marini F, Krause D, et al. Minimal criteria for defining multipotent mesenchymal stromal cells. The International Society for Cellular Therapy position statement. Cytotherapy 2006;8(4):315–7.

[29] Kono S, Kazama T, Kano K, Harada K, Uechi M, Matsumoto T. Phenotypic and functional properties of feline dedifferentiated fat cells and adipose-derived stem cells. Vet J 2014;199(1):88–96.
[30] Tangchitphisut P, Srikaew N, Numhom S, Tangprasittipap A, Woratanarat P, Wongsak S, et al. Infrapatellar fat pad: an alternative source of adipose-derived mesenchymal stem cells. Arthritis 2016;2016:4019873.
[31] Lee MJ, Wu Y, Fried SK. Adipose tissue heterogeneity: implication of depot differences in adipose tissue for obesity complications. Mol Aspects Med 2013;34(1):1–11.
[32] Garcia J, Mennan C, McCarthy HS, Roberts S, Richardson JB, Wright KT. Chondrogenic potency analyses of donor-matched chondrocytes and mesenchymal stem cells derived from bone marrow, infrapatellar fat pad, and subcutaneous fat. Stem Cells Int 2016;2016:6969726.
[33] Neri S, Guidotti S, Lilli NL, Cattini L, Mariani E. Infrapatellar fat pad-derived mesenchymal stromal cells from osteoarthritis patients: in vitro genetic stability and replicative senescence. J Orthop Res 2017;35(5):1029–37.
[34] Zhong YC, Wang SC, Han YH, Wen Y. Recent advance in source, property, differentiation, and applications of infrapatellar fat pad adipose-derived stem cells. Stem Cells Int 2020;2020:2560174.
[35] Tsurumachi N, Akita D, Kano K, Matsumoto T, Toriumi T, Kazama T, et al. Small buccal fat pad cells have high osteogenic differentiation potential. Tissue Eng Part C Methods 2016;22(3):250–9.